

Article

Heteroatom (Nitrogen/Sulfur)-Doped Graphene as an Efficient Electrocatalyst for Oxygen Reduction and Evolution Reactions

Jian Zhang ¹, Jia Wang ², Zexing Wu ², Shuai Wang ^{2,*} , Yumin Wu ^{1,*} and Xien Liu ² 

¹ College of Chemical Engineering, Qingdao University of Science & Technology, Qingdao 266042, China; jian8552@163.com

² State Key Laboratory Base of Eco-Chemical Engineering, College of Chemistry and Molecular Engineering, Qingdao University of Science & Technology, Qingdao 266042, China; wangjia3588@163.com (J.W.); splswzx@qust.edu.cn (Z.W.); liuxien@qust.edu.cn (X.L.)

* Correspondence: qustwangshuai@qust.edu.cn (S.W.); wuyumin001@126.com (Y.W.); Tel.: +86-150-9202-5911 (S.W.); +86-138-5463-8500 (Y.W.)

Received: 10 September 2018; Accepted: 18 October 2018; Published: 19 October 2018



Abstract: Carbon nanomaterials are potential materials with their intrinsic structure and property in energy conversion and storage. As the electrocatalysts, graphene is more remarkable in electrochemical reactions. Additionally, heteroatoms doping with metal-free materials can obtain unique structure and demonstrate excellent electrocatalytic performance. In this work, we proposed a facile method to prepare bifunctional electrocatalyst which was constructed by nitrogen, sulfur doped graphene (NSG), which demonstrate superior properties with high activity and excellent durability compared with Pt/C and IrO₂ for oxygen reduction (OR) and oxygen evolution (OE) reactions. Accordingly, these phenomena are closely related to the synergistic effect of doping with nitrogen and sulfur by rationally regulating the polarity of carbon in graphene. The current work expands the method towards carbon materials with heteroatom dopants for commercialization in energy-related reactions.

Keywords: electrocatalysts; bifunctional catalyst; graphene; dopants

1. Introduction

Graphene, a two-dimensional atom-thick conjugated structure, has drawn particular attention for its good conductivity, mechanical property, electrochemical stability and huge specific surface area as well as its wide potential applications in catalysts [1,2]. However, graphene oxide has serious structure disorder and contains oxygen-containing groups, which weaken its electrode transportation and conductivity [3–6]. Heteroatoms like N and S are adjacent elements to carbon. The doping of such elements to graphene may change its structure and improve the electrochemical property of graphene [4,7–10] due to its excellent stability, durability and controllability of nanoparticles [11,12].

On the other hand, fuel cells and metal-air batteries, as promising high-performance electrochemical energy-related devices, are suffering from bottlenecks because of its sluggish kinetics in oxygen reduction reaction (ORR, $O_2 + H_2O + 4e^- \rightarrow 4OH^-$) [13–18]. The platinum (Pt), with the advantage of low overpotential and high current density, has been served as the most promising ORR electrocatalyst regardless of the scarcity, high cost, and poor durability which obstruct its application in the energy field [7,19–22]. To address this problem, seeking alternative ORR and OER electrocatalysts with low overpotentials and cost is urgent for sustainable energy solutions. Heteroatom doped carbon-based materials as promising metal-free electrocatalysts have encouraged intensive research, while it is found that, the hybrids of doped graphene show multi-functions, and have a wide application

prospect in energy storage and conversion and environmental detection. They can be used as catalysts for ORR and OER, but the relationship between precursor-doping pattern-ORR activity remains unclear [16,23–26]. Additionally, the performance of ORR and OER of some metal-free electrocatalysts can be optimized. Therefore, developing low cost and high electrocatalytic efficiency metal-free materials has become a focus of study.

Herein, we developed an efficient method to prepare heteroatom nitrogen-, sulfur-doped graphene as bifunctional materials for ORR/OER by hydrothermal synthesis of graphene oxide and potassium thiocyanate (KSCN), whether the guest gas (NH_3) exists or not.

2. Results and Discussion

2.1. Characterization of Electrocatalysts

The structure and morphology of materials were investigated through scanning electron microscopy (SEM) and transmission electron microscopy (TEM) [27]. As observed in Figure 1 and Figure S1, the elements of C, N, O and S were distributed uniformly in NSG, with the fabrication of stacking graphene sheets. This specific morphology could catalyze the reaction process derived from the exposing of more active sites. The SEM analyses (Figure 1b) confirm that the heteroatoms were doped successfully. The microstructure of nitrogen doped graphene (NG) and sulfur doped graphene (SG) were shown in Figures S2 and S3 where the twisted graphene layers were clearly observed.

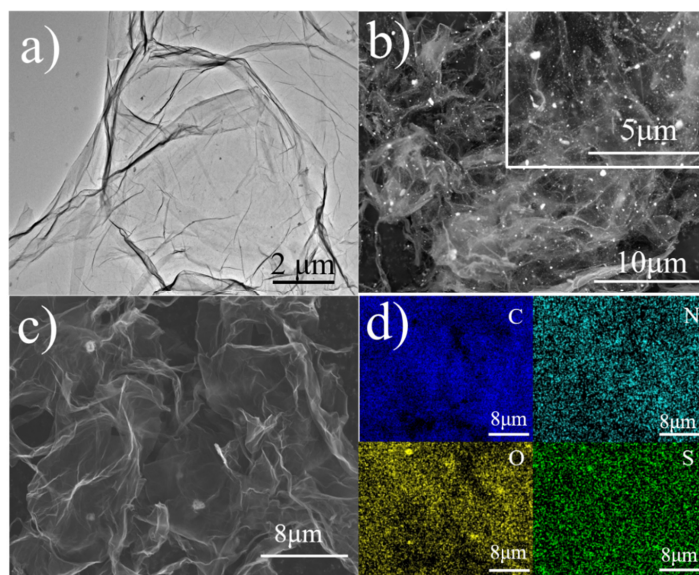


Figure 1. Transmission electron microscopy (TEM) (a), scanning electron microscopy (SEM) (b,c) and mapping (d) of C, N, O, S for NSG.

X-ray photoelectron spectroscopy (XPS) tests were the valid method to analyze the ingredients and chemical valence of materials [28]. As shown in Figure 2a, Compositions of C, N, O and S were evaluated through XPS survey spectrum whose atomic percentages respectively are 91.90, 4.18, 3.90 and 0.02 at %, demonstrating the successful doping with nitrogen and sulfur. As observed from Figure 2b, sp^2 hybridized graphitic carbon, C–S and C=O and C=N were corresponding to 284.5 eV, 285.5 eV and 287.0 eV, respectively. Pyridinic N (397.8 eV), pyrrolic N (398.9 eV) and graphitic N (400.3 eV) all existed (Figure 2c). As we know, graphitic N is viewed as active sites in the oxygen reduction reaction [23,28]. Moving to Figure 2d, high resolution S 2p, the peaks of 163.9 and 165.0 eV can ascribe to the S 2p spin-orbit doublet (S 2p_{1/2} and S 2p_{3/2}) [29], affected by C–S–C, deeply demonstrating the successful addition with sulfur [30]. Compared with the high resolution N 1s of NG (Figure S4), the existence of C–S–C and synergistic effects of N and S doping may be the essential factors of

performance improvement for NSG. All of this demonstrated the synergy of N and S catalyzed the activity of NSG.

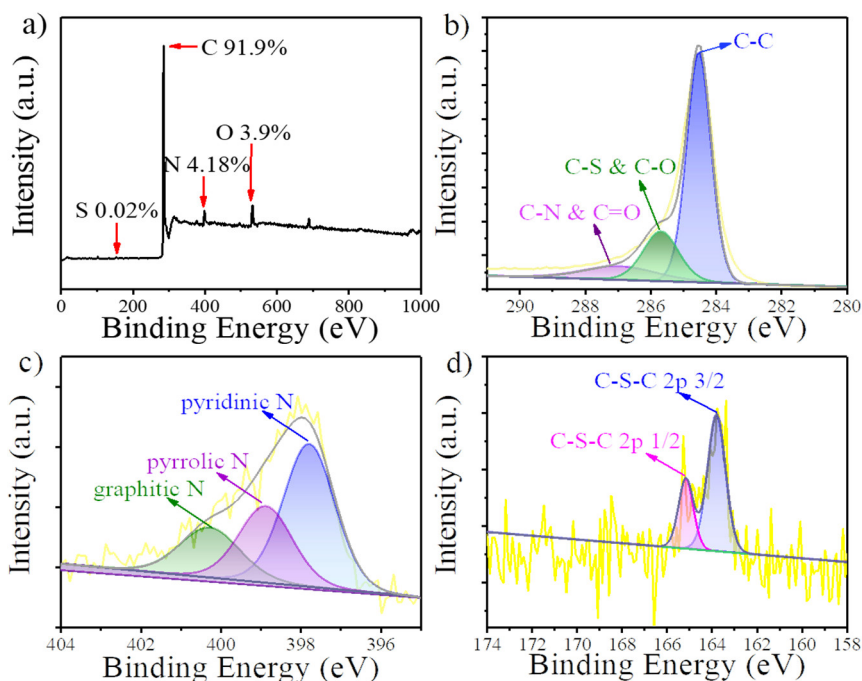


Figure 2. (a) Full range XPS spectra of NSG; (b–d) XPS spectrum of C 1s, N 1s and S 2p for NSG.

Figure 3a shows distinct Raman spectra at 1345 and 1600 cm^{-1} which is ascribed to the D and G band. A recent report indicated that the G band represents the graphitization degree of materials, structural defects are reflected by the D band [31]. To our best knowledge, the I_D/I_G ratio represents structural disorder in graphitic materials [32]. As observed from Figure 3a, the value of NSG (1.09) was lower than that of SG (1.15) and NG (1.29), indicating the increasing graphitic degree of NSG which may be derived from the “self-repairing” of intermediate products under experimental conditions with the repairing of partial sp^2 -bonded C atoms. The components of the electrocatalysts were also analyzed. The graphitic C structure existed in NSG, SG and NG at 24° with the observation of X-ray diffraction (XRD) spectrum in Figure 3b [33]. In addition, for SG and NSG, the inconspicuous peak at 667 cm^{-1} belonged to the vibration of C–S bond which was making a clear indication that S element was doped with graphene in Figure S5 [5,8].

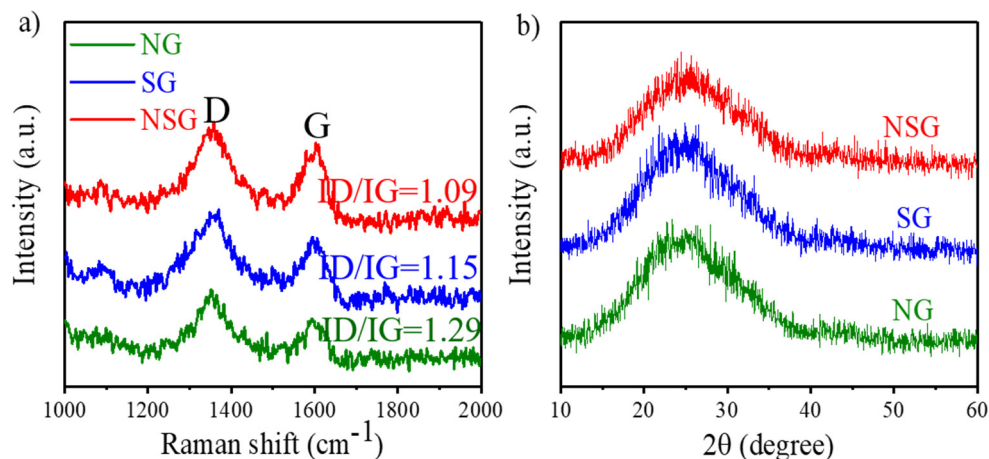


Figure 3. Raman spectra (a) and X-ray diffraction (XRD) (b) of NSG, NG and SG.

2.2. Electrocatalytic Properties of Catalysts

In O₂-saturated 0.1 M KOH electrolyte, a usual three-electrode electrochemical device consisted of Ag/AgCl, Pt wire and rotating ring-disk electrode (4 mm diameter) which was orderly used as a reference electrode, counter electrode and working electrode with the continuous flowing of O₂ operated to test the ORR performances of different catalysts which was revealed by linear sweep voltammetry (LSV) [34]. According to the conversion equation ($V_{\text{RHE}} = V_{\text{Ag/AgCl}} + 0.059\text{pH} + 0.197$), the potentials tested through Ag/AgCl were converted into reversible hydrogen electrode (RHE).

Compared with commercial Pt/C (20 wt %), the ORR performance of NSG, SG and NG was investigated via LSV in 0.1 M KOH electrolyte (Figure 4a). Obviously, NSG shows higher onset potential (0.95 V vs. RHE) compared with SG and NG (0.90 and 0.89 V). For half-wave potential, as shown in Figure 4b, the value of NSG (0.84 V) is prior to that of Pt/C, SG and NG (0.82, 0.8, 0.77 V), indicating its preponderant electrocatalytic performance for ORR. In addition, NSG displays large limited current density, demonstrating a more efficient mass transfer among such electrocatalysts [5].

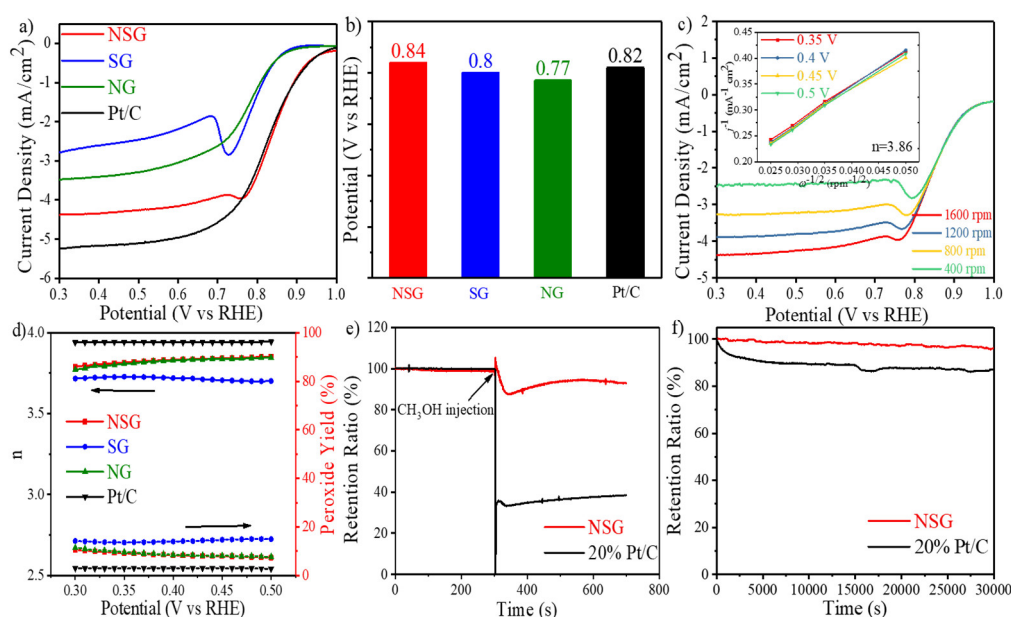


Figure 4. (a) Oxygen reduction reaction (ORR) polarization curves of Pt/C, NSG, SG, NG in O₂-saturated 0.1 M KOH solution, respectively (rotation speed 1600 rpm, sweep rate 10 mV s⁻¹); (b) Half-wave potential of NSG, SG, NG and Pt/C; (c) ORR polarization curves of NSG at the various rotation speeds (sweep rate 10 mV s⁻¹) (inset: Corresponding K-L plots at different electrode potentials); (d) The electron transfer number *n* of NSG, NG, SG and Pt/C at different potentials (left), and percentage (%) of peroxide with respect to the total oxygen reduction products (right); (e) Chronoamperometric response of NSG and 20% Pt/C at 0.57 V in O₂-saturated 0.1 mol L⁻¹ KOH solution. The arrows indicate the addition of methanol; (f) Durability evaluation of NSG and 20% Pt/C at 0.57 V for 30,000 s with a rotating rate of 1600 rpm.

In order to quantitatively analyze the mechanism of synthesized catalysts for ORR, further LSVs were recorded at 400, 800, 1200 and 1600 rpm (Figure 4c, Figure S6a,c). Koutecky-Levich (K-L) plots were illustrated in Figure 4c and Figure S5b,d. To the best of our knowledge, a function relationship exists between inverse current density and square root of the rotation rate at a different range of potentials. According to the calculating formula of K-L equation, 3.86, 3.72 and 3.73, the electron transfer numbers (*n*) of NSG, SG and NG, indicate the ORRs mechanism is a four-electron process.

To further explore the performance of synthesized electrocatalysts, the electron transfer number (*n*) and percentage (%) of peroxide species were tested through a rotating ring disk electrode (RRDE). As shown in Figure 4d, the four-electron process of the as-prepared NSG for ORR is consistent with the

RDE results. Additionally the average percentage (%) of peroxide yield of NSG is the lowest compared with SG and NG, demonstrating the multiple doping.

Adding 8.5 mL methanol into 70 mL 0.1 M KOH electrolyte with continuous O₂, the tolerance of NSG to methanol was investigated. Compared with the sharp decline of current density of Pt/C (current loss of ~60%), NSG exhibits a little fluctuation with a retention ratio of ~93%, demonstrating the decreased activity of Pt/C affected by methanol, and NSG possesses a well tolerance to methanol (Figure 4e).

As a state-of-the-art catalyst for ORR, chronoamperometric measurement was used to assess the durability at a constant cathodic voltage of 0.57 V. As observed from Figure 4f, NSG exhibits an outstanding ORR stability with a weak attenuation over 30,000 s, maintaining 96% of the initial current. Compared with approximately 15% loss of initial current, NSG was better than Pt/C for ORR in alkaline electrolyte. OER activity of various as-prepared samples was also tested in the same condition (Figure 5a). To our best knowledge, the quantitative value of $E_j = 10$ (potentials to deliver 10 mA cm⁻² current density) represents 10% efficient solar water-splitting cell which is used to make comparison with various catalysts [35]. For NSG, $E_j = 10$ (1.62 V) is lower than that of 1.65 V (SG), 1.66 V (NG) and some of state-of-the-art carbon-based catalysts, just like N, S-CN [5] and CN nanocables [36] and so on. The Tafel slope of NSG (105 mV dec⁻¹) is lower than that of SG (121 mV dec⁻¹) and NG (124 mV dec⁻¹), indicating its favorable reaction kinetics (Figure 5b). In addition, the representation of charge transfer kinetics, electrochemical impedance spectroscopy (EIS) of NSG, NG and SG, were also investigated. The Nyquist plots in Figure S7 demonstrates a lower charge transfer resistance towards the OER process of NSG than that of NG and SG, which is consistent with the OER performance, revealing faster Faradaic process in OER kinetics of NSG.

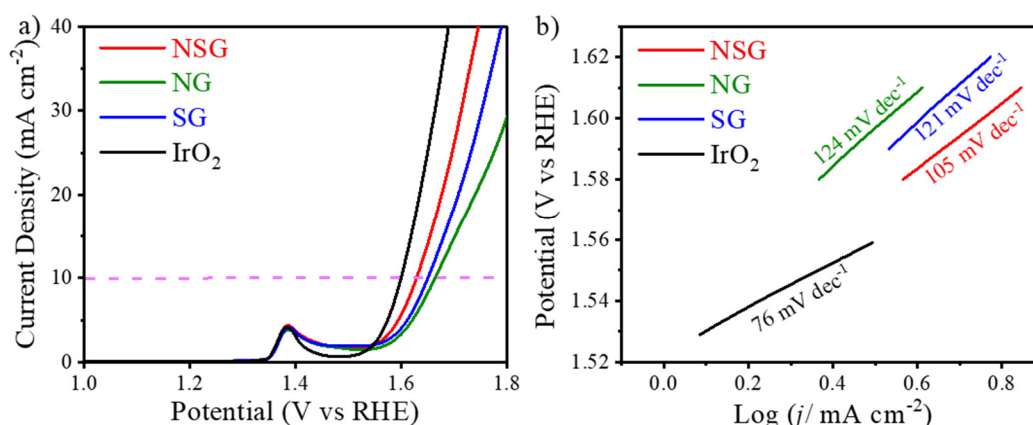


Figure 5. (a) OER linear sweeping voltammeters (LSVs) of NG, SG, IrO₂ and NSG at a sweep rate of 10 mV s⁻¹; (b) OER Tafel plots.

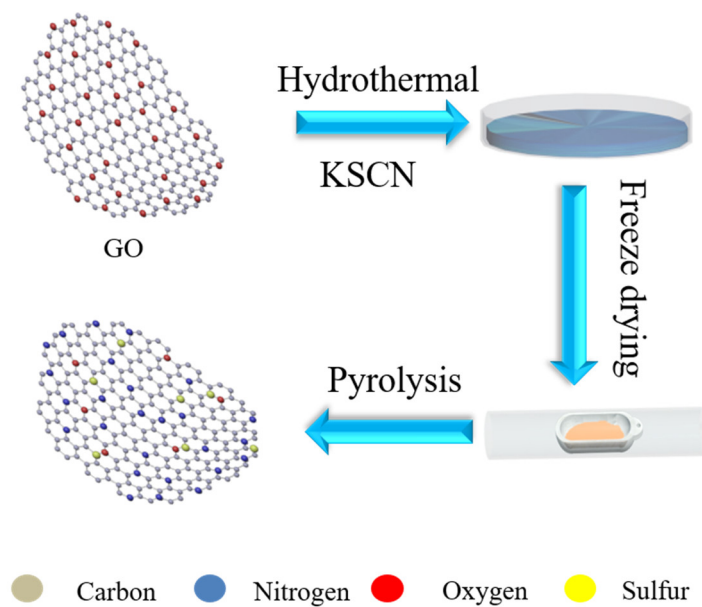
Considering the structure-property relationship, the better catalytic performance towards ORR and OER may be a result of the stable covalent C–N which could form high positive charge density on neighboring carbon atoms, and the mismatch of outermost orbitals between C and S [37] and large surface area [38] which could facilitate the charge transfer, further endowing more accessible catalytic surfaces.

3. Materials and Methods

3.1. Preparation of Electrocatalysts

At first, GO was prepared according to the procedure used by Hummer [39]. To begin this process, GO and KSCN (20.0 mg/20.0 mg) were intensively mixed in 30.0 mL deionized water. Then, a homogeneous solution was fabricated through ultrasonication and kept in Teflon-lined stainless-steel autoclave (150 °C) for 15 h. The as-prepared solution was treated, at freezing, with a

vacuum dryer overnight to form powder. After dried, the powder was placed in a tube furnace which was programmed at 800 °C for 2 h with 5 °C/min of rising rate, keeping Ar flowing of 150 mL/min. In the end, with Ar and NH₃ whose flow rate is 500 mL/min, the intermediate product was annealed at 800 °C for 1 h (Scheme 1). Up to now, the target materials were obtained and defined as nitrogen-, sulfur- co-doped graphene (NSG). For the sake of contrast, only S-doped or N-doped graphene catalysts were synthesized under the same operating conditions which was defined as SG or NG, respectively. In other words, the only source of N (NH₃) or S (KSCN) was used as introduction.



Scheme 1. Schematic illustration of the preparation of NSG.

3.2. Characterization of Electrocatalysts

A S-4800 SEM instrument (Hitachi High-Technology Co., Ltd., Tokyo, Japan) was used to test the surface characterization of different electrocatalysts. TEM (JEOL JEM-2100, Tokyo, Japan) was operated at 200 kV. With radiation of Cu-K α , X-ray diffraction (XRD, D/Max2000, Rigaku, Japan) was investigated. Fourier transformed infrared (FTIR) spectra were observed through a TENSOR 27 FT-IR spectrometer (Scotia, NY, USA) in the range of 4000–500 cm⁻¹, after the samples were dried. Escalab 250 xi (Thermo Scientific, Loughborough, UK) was used to record X-ray photoelectron spectroscopy (XPS), providing a base pressure of 5×10^{-9} Torr radiated from monochromatic Al K α . Raman spectra were investigated by using a Renishaw Raman spectroscopy (Renishaw plc., Gloucestershire, UK).

4. Conclusions

To conclude this work, the four-electron pathway for ORR on N, S-co-doped graphene is revealed and synergy effects between dopants are discussed. The synergy effect is ascribed to the increasing spin density with the dopant of S and graphitic N. The as-prepared catalyst exhibits excellent performance for ORR and OER which is originated from the unique structure of NSG, fortunately, the unique structure is to the benefit of mass transfer. Overall, this work provides a carbon-based bifunctional electrocatalyst of dual doping in ORR and OER on the promising widespread application in energy-related devices.

Supplementary Materials: The following are available online at <http://www.mdpi.com/2073-4344/8/10/475/s1>, Figure S1: Energy dispersive spectrometer (EDS) of NSG, Figure S2: SEM (a-c) and mapping of C (d), N (e), O (f) of NG, Figure S3: SEM (a,b) and mapping of C (c), N (d), O (e) and S (f) of SG, Figure S4: Full range XPS spectra of NG, XPS spectrum of C 1s and N 1s for NG, Figures S5: Fourier transform infrared spectroscopy (FTIR) of NSG,

SG, NG and GO, Figure S6: (a,c) Linear Scan Voltammetry (LSV) curves for SG and NG at different rotation rates in 0.1 M KOH. (b,d) Corresponding K-L plots at different potentials: 0.35, 0.4, 0.45, 0.5 V, Figure S7: Nyquist plots of electrochemical impedance spectra (EIS) of NSG, SG and NG recorded in 1 M KOH. Inset: One-time-constant model equivalent circuit used for data fitting of EIS spectra, Table S1: Comparison of ORR and OER performance of NSG with the recently reported metal-free catalysts at 1600 rpm in KOH solution.

Author Contributions: Data curation, J.Z.; Project administration, X.L.; Software, J.W.; Supervision, Z.W.; Writing—original draft, S.W.; Writing—review and editing, Y.W.

Funding: This research was funded by Taishan Scholar Program of Shandong Province, China (ts201712045). The Key Research and Development Program of Shandong Province (2018GGX104001). Natural Science Foundation of Shandong Province of China (ZR2017MB054). Doctoral Fund of QUST (0100229001). Post-doctoral Applied Research Fund of Qingdao (04000641). (†, equally contribution).

Conflicts of Interest: The authors declare no conflict of interest.

References

1. Higgins, D.; Hoque, M.A.; Seo, M.H.; Wang, R.; Hassan, F.; Choi, J.-Y.; Pritzker, M.; Yu, A.; Zhang, J.; Chen, Z. Development and simulation of sulfur-doped graphene supported platinum with exemplary stability and activity towards oxygen reduction. *Adv. Funct. Mater.* **2014**, *24*, 4325–4336. [[CrossRef](#)]
2. Ge, X.; Sumboja, A.; Wu, D.; An, T.; Li, B.; Goh, F.W.T.; Hor, T.S.A.; Zong, Y.; Liu, Z. Oxygen reduction in alkaline media: From mechanisms to recent advances of catalysts. *ACS Catal.* **2015**, *5*, 4643–4667. [[CrossRef](#)]
3. Han, J.H.; Huang, G.; Wang, Z.L.; Lu, Z.; Du, J.; Kashani, H.; Chen, M.W. Low temperature carbide-mediated growth of bicontinuous nitrogen-doped mesoporous graphene as an efficient oxygen reduction electrocatalyst. *Adv. Mater.* **2018**, *30*, 1803588. [[CrossRef](#)] [[PubMed](#)]
4. Li, J.; Zhang, Y.; Zhang, X.; Huang, J.; Han, J.; Zhang, Z.; Han, X.; Xu, P.; Song, B.S. N dual-doped graphene-like carbon nanosheets as efficient oxygen reduction reaction electrocatalysts. *ACS Appl. Mater. Interfaces* **2017**, *9*, 398–405. [[CrossRef](#)] [[PubMed](#)]
5. Qu, K.; Zheng, Y.; Dai, S.; Qiao, S.Z. Graphene oxide-polydopamine derived n, s-codoped carbon nanosheets as superior bifunctional electrocatalysts for oxygen reduction and evolution. *Nano Energy* **2016**, *19*, 373–381. [[CrossRef](#)]
6. Sakthinathan, S.; Kubendhiran, S.; Chen, S.-M.; Karuppiyah, C.; Chiu, T.-W. Novel bifunctional electrocatalyst for orr activity and methyl parathion detection based on reduced graphene oxide/palladium tetraphenylporphyrin nanocomposite. *J. Phys. Chem. C* **2017**, *121*, 14096–14107. [[CrossRef](#)]
7. Wu, J.; Ma, L.; Yadav, R.M.; Yang, Y.; Zhang, X.; Vajtai, R.; Lou, J.; Ajayan, P.M. Nitrogen-doped graphene with pyridinic dominance as a highly active and stable electrocatalyst for oxygen reduction. *ACS Appl. Mater. Interfaces* **2015**, *7*, 14763–14769. [[CrossRef](#)] [[PubMed](#)]
8. Akhter, T.; Islam, M.M.; Faisal, S.N.; Haque, E.; Minett, A.I.; Liu, H.K.; Konstantinov, K.; Dou, S.X. Self-assembled n/s codoped flexible graphene paper for high performance energy storage and oxygen reduction reaction. *ACS Appl. Mater. Interfaces* **2016**, *8*, 2078–2087. [[CrossRef](#)] [[PubMed](#)]
9. Men, B.; Sun, Y.; Liu, J.; Tang, Y.; Chen, Y.; Wan, P.; Pan, J. Synergistically enhanced electrocatalytic activity of sandwich-like n-doped graphene/carbon nanosheets decorated by fe and s for oxygen reduction reaction. *ACS Appl. Mater. Interfaces* **2016**, *8*, 19533–19541. [[CrossRef](#)] [[PubMed](#)]
10. Khilari, S.; Pradhan, D. Mnfe2o4@nitrogen-doped reduced graphene oxide nanohybrid: An efficient bifunctional electrocatalyst for anodic hydrazine oxidation and cathodic oxygen reduction. *Catal. Sci. Technol.* **2017**, *7*, 5920–5931. [[CrossRef](#)]
11. Alshehri, S.M.; Alhabarah, A.N.; Ahmed, J.; Naushad, M.; Ahamad, T. An efficient and cost-effective tri-functional electrocatalyst based on cobalt ferrite embedded nitrogen doped carbon. *J. Colloid Interface Sci.* **2018**, *514*, 1–9. [[CrossRef](#)] [[PubMed](#)]
12. Alshehri, S.M.; Ahmed, J.; Ahamad, T.; Alhokbany, N.; Arunachalam, P.; Almayouf, A.M.; Ahmad, T. Synthesis, characterization, multifunctional electrochemical (OGR/ORR/SCs) and photodegradable activities of ZnWO₄ nanobricks. *J. Sol-Gel Sci. Technol.* **2018**, *87*, 137–146. [[CrossRef](#)]
13. Hoque, M.A.; Hassan, F.M.; Higgins, D.; Choi, J.Y.; Pritzker, M.; Knights, S.; Ye, S.; Chen, Z. Multigrain platinum nanowires consisting of oriented nanoparticles anchored on sulfur-doped graphene as a highly active and durable oxygen reduction electrocatalyst. *Adv. Mater.* **2015**, *27*, 1229–1234. [[CrossRef](#)] [[PubMed](#)]

14. Li, Y.; Gong, M.; Liang, Y.; Feng, J.; Kim, J.E.; Wang, H.; Hong, G.; Zhang, B.; Dai, H. Advanced zinc-air batteries based on high-performance hybrid electrocatalysts. *Nat. Commun.* **2013**, *4*, 1805. [[CrossRef](#)] [[PubMed](#)]
15. Lv, Y.; Wang, X.; Mei, T.; Li, J.; Wang, J. Single-step hydrothermal synthesis of n, s-dual-doped graphene networks as metal-free efficient electrocatalysts for oxygen reduction reaction. *ChemistrySelect* **2018**, *3*, 3241–3250. [[CrossRef](#)]
16. Gaidukevič, J.; Razumienė, J.; Šakinytė, I.; Rebelo, S.L.H.; Barkauskas, J. Study on the structure and electrocatalytic activity of graphene-based nanocomposite materials containing (SCN)_n. *Carbon* **2017**, *118*, 156–167. [[CrossRef](#)]
17. Song, J.; Liu, T.; Ali, S.; Li, B.; Su, D. The synergy effect and reaction pathway in the oxygen reduction reaction on the sulfur and nitrogen dual doped graphene catalyst. *Chem. Phys. Lett.* **2017**, *677*, 65–69. [[CrossRef](#)]
18. Alshehri, S.M.; Ahmed, J.; Ahamad, T.; Arunachalam, P.; Ahmad, T.; Khan, A. Bifunctional electro-catalytic performances of CoWO₄ nanocubes for water redox reactions (OER/ORR). *RSC Adv.* **2017**, *7*, 45615–45623. [[CrossRef](#)]
19. Ghanem, M.A.; Arunachalam, P.; Almayouf, A.; Weller, M.T. Efficient Bi-Functional Electrocatalysts of Strontium Iron Oxy-Halides for Oxygen Evolution and Reduction Reactions in Alkaline Media. *J. Electrochem. Soc.* **2016**, *163*, H450–H458. [[CrossRef](#)]
20. Chang, Y.; Hong, F.; He, C.; Zhang, Q.; Liu, J. Nitrogen and sulfur dual-doped non-noble catalyst using fluidic acrylonitrile telomer as precursor for efficient oxygen reduction. *Adv. Mater.* **2013**, *25*, 4794–4799. [[CrossRef](#)] [[PubMed](#)]
21. Wang, L.; Ambrosi, A.; Pumera, M. “Metal-free” catalytic oxygen reduction reaction on heteroatom-doped graphene is caused by trace metal impurities. *Angew. Chem. Int. Ed.* **2013**, *52*, 13818–13821. [[CrossRef](#)] [[PubMed](#)]
22. Wang, N.; Lu, B.; Li, L.; Niu, W.; Tang, Z.; Kang, X.; Chen, S. Graphitic nitrogen is responsible for oxygen electroreduction on nitrogen-doped carbons in alkaline electrolytes: Insights from activity attenuation studies and theoretical calculations. *ACS Catal.* **2018**, *8*, 6827–6836. [[CrossRef](#)]
23. Chai, G.-L.; Qiu, K.; Qiao, M.; Titirici, M.-M.; Shang, C.; Guo, Z. Active sites engineering leads to exceptional orr and oer bifunctionality in p,n co-doped graphene frameworks. *Energy Environ. Sci.* **2017**, *10*, 1186–1195. [[CrossRef](#)]
24. Chenitz, R.; Kramm, U.I.; Lefèvre, M.; Glibin, V.; Zhang, G.; Sun, S.; Dodelet, J.-P. A specific demetalation of Fe–N₄ catalytic sites in the micropores of NC_Ar + NH₃ is at the origin of the initial activity loss of the highly active Fe/N/C catalyst used for the reduction of oxygen in pem fuel cells. *Energy Environ. Sci.* **2018**, *11*, 365–382. [[CrossRef](#)]
25. Hassani, S.S.; Samiee, L.; Ghasemy, E.; Rashidi, A.; Ganjali, M.R.; Tasharrofi, S. Porous nitrogen-doped graphene prepared through pyrolysis of ammonium acetate as an efficient orr nanocatalyst. *Int. J. Hydrogen Energy* **2018**, *43*, 15941–15951. [[CrossRef](#)]
26. Kumar, K.; Canaff, C.; Rousseau, J.; Arrii-Clacens, S.; Napporn, T.W.; Habrioux, A.; Kokoh, K.B. Effect of the oxide–carbon heterointerface on the activity of Co₃O₄/nrngo nanocomposites toward ORR and OER. *J. Phys. Chem. C* **2016**, *120*, 7949–7958. [[CrossRef](#)]
27. Higgins, D.; Zamani, P.; Yu, A.; Chen, Z. The application of graphene and its composites in oxygen reduction electrocatalysis: A perspective and review of recent progress. *Energy Environ. Sci.* **2016**, *9*, 357–390. [[CrossRef](#)]
28. Yan, P.; Liu, J.; Yuan, S.; Liu, Y.; Cen, W.; Chen, Y. The promotion effects of graphitic and pyridinic n combinational doping on graphene for orr. *Appl. Surf. Sci.* **2018**, *445*, 398–403. [[CrossRef](#)]
29. Li, F.; Sun, L.; Luo, Y.; Li, M.; Xu, Y.; Hu, G.; Li, X.; Wang, L. Effect of thiophene s on the enhanced orr electrocatalytic performance of sulfur-doped graphene quantum dot/reduced graphene oxide nanocomposites. *RSC Adv.* **2018**, *8*, 19635–19641. [[CrossRef](#)]
30. Hoque, M.A.; Hassan, F.M.; Jauhar, A.M.; Jiang, G.; Pritzker, M.; Choi, J.-Y.; Knights, S.; Ye, S.; Chen, Z. Web-like 3d architecture of pt nanowires and sulfur-doped carbon nanotube with superior electrocatalytic performance. *ACS Sustain. Chem. Eng.* **2017**, *6*, 93–98. [[CrossRef](#)]
31. Chen, S.; Duan, J.; Jaroniec, M.; Qiao, S.Z. Nitrogen and oxygen dual-doped carbon hydrogel film as a substrate-free electrode for highly efficient oxygen evolution reaction. *Adv. Mater.* **2014**, *26*, 2925–2930. [[CrossRef](#)] [[PubMed](#)]

32. Lei, W.; Liu, S.; Zhang, W.-H. Porous hollow carbon nanofibers derived from multi-walled carbon nanotubes and sucrose as anode materials for lithium-ion batteries. *RSC Adv.* **2017**, *7*, 224–230. [[CrossRef](#)]
33. Cazetta, A.L.; Zhang, T.; Silva, T.L.; Almeida, V.C.; Asefa, T. Bone char-derived metal-free n- and s-co-doped nanoporous carbon and its efficient electrocatalytic activity for hydrazine oxidation. *Appl. Catal. B Environ.* **2018**, *225*, 30–39. [[CrossRef](#)]
34. Xu, C.; Xu, B.; Gu, Y.; Xiong, Z.; Sun, J.; Zhao, X.S. Graphene-based electrodes for electrochemical energy storage. *Energy Environ. Sci.* **2013**, *6*, 1388. [[CrossRef](#)]
35. Paulraj, A.; Kiros, Y.; Göthelid, M.; Johansson, M. Nifeox as a bifunctional electrocatalyst for oxygen reduction (OR) and evolution (OE) reaction in alkaline media. *Catalysts* **2018**, *8*, 328. [[CrossRef](#)]
36. Tian, G.-L.; Zhang, Q.; Zhang, B.; Jin, Y.-G.; Huang, J.-Q.; Su, D.S.; Wei, F. Toward full exposure of “active sites”: Nanocarbon electrocatalyst with surface enriched nitrogen for superior oxygen reduction and evolution reactivity. *Adv. Funct. Mater.* **2014**, *24*, 5956–5961. [[CrossRef](#)]
37. Huang, H.; Ma, L.; Tiwary, C.S.; Jiang, Q.; Yin, K.; Zhou, W.; Ajayan, P.M. Worm-shape pt nanocrystals grown on nitrogen-doped low-defect graphene sheets: Highly efficient electrocatalysts for methanol oxidation reaction. *Small* **2017**, *13*, 1603013. [[CrossRef](#)]
38. Qiao, X.; Jin, J.; Fan, H.; Cui, L.; Ji, S.; Li, Y.; Liao, S. Cobalt and nitrogen co-doped graphene-carbon nanotube aerogel as an efficient bifunctional electrocatalyst for oxygen reduction and evolution reactions. *Catalysts* **2018**, *8*, 275. [[CrossRef](#)]
39. Yang, Q.; Su, Y.; Chi, C.; Cherian, C.T.; Huang, K.; Kravets, V.G.; Wang, F.C.; Zhang, J.C.; Pratt, A.; Grigorenko, A.N.; et al. Ultrathin graphene-based membrane with precise molecular sieving and ultrafast solvent permeation. *Nat. Mater.* **2017**, *16*, 1198–1202. [[CrossRef](#)] [[PubMed](#)]



© 2018 by the authors. Licensee MDPI, Basel, Switzerland. This article is an open access article distributed under the terms and conditions of the Creative Commons Attribution (CC BY) license (<http://creativecommons.org/licenses/by/4.0/>).